Phytochemistry 69 (2008) 2689–2695

Contents lists available at ScienceDirect

Phytochemistry

journal homepage: www.elsevier.com/locate/phytochem

# NMR characterization of hydration and thermal stress in tomato fruit cuticles

Ruth E. Stark [a,b,*], Bin Yan [a], Suzanne M. Stanley-Fernandez [a], Zhen-jia Chen [a], Joel R. Garbow [c,d]

[a] Department of Chemistry, College of Staten Island, City University of New York Graduate Center and Institute for Macromolecular Assemblies, New York, NY 10031, USA
[b] Department of Chemistry, City College of New York, City University of New York Graduate Center and Institute for Macromolecular Assemblies, 160 Convent Avenue, New York, NY 10031, USA
[c] Department of Chemistry, Washington University in St. Louis, St. Louis, MO 63130, USA
[d] Department of Radiology, Biomedical Magnetic Resonance Laboratory, Washington University in St. Louis, St. Louis, MO 63110, USA

ARTICLE INFO

*Article history:*
Received 17 May 2008
Received in revised form 16 August 2008
Available online 8 October 2008

*Keywords:*
*Lycopersicon esculentum*
Solanaceae
Tomato
Fruit
Cuticle
Plant cuticle
Polyester
Hydration stress
Temperature stress
NMR
Solid-state NMR
C-13 NMR
CPMAS
Spin relaxation
Molecular dynamics

ABSTRACT

In its natural environment, the plant cuticle, which is composed of the biopolymer cutin and a mixture of surface and embedded cuticular waxes, experiences a wide variety of temperatures and hydration states. Consequently, a complete understanding of cuticular function requires study of its thermal and mechanical properties as a function of hydration. Herein, we report the results of a comprehensive $^{13}C$ nuclear magnetic resonance (NMR) relaxation study of hydrated tomato fruit cuticle. Cross-polarization and direct-polarization experiments serve to measure the solid-like and liquid-like components, respectively, of hydrated cuticle. Localized, high-frequency motions are probed by $T_1(C)$ spin relaxation measurements, whereas $T_{1\rho}(H)$ and $T_{1\rho}(C)$ experiments reflect low-frequency, lower amplitude polymer-chain motions. In addition, variable-temperature measurements of $T_1(C)$ and $T_{1\rho}(C)$ for dry tomato cuticles are used to evaluate the impact of temperature stress. Results of these experiments are interpreted in terms of changes occurring in individual polymer motions of the cutin/wax components of tomato cuticle and in the interaction of these components within intact cuticle, both of which are expected to influence the functional integrity of this protective plant covering.



## 1. Introduction

The aerial surfaces of the leaves and fruit of terrestrial plants consist of a cuticular barrier that covers the outer 0.1–10 μm of the plant surface. The cuticle controls the plant's interactions with the environment, protects against water loss, and functions as the plant's primary protective barrier against pathogenic attack (Heredia, 2003). Fruit cuticles may also be considered as smart surfaces – they exhibit spatially selective self-cleaning capabilities and developmentally sensitive mechanical performance (Bargel et al., 2006). The cuticular structure is composed of two primary components: an amorphous polymerized (polyester) network of hydroxylated fatty acids, known as cutin, and a lipid mixture comprised of various waxes (predominantly long chain, $\sim C_{30}$ aliphatic-based hydrocarbons) for waterproofing. A thin layer of epicuticular lipids coats the outer surface of the cuticle, whereas intracuticular lipids are typically embedded within the cutin matrix. Using chemical degradation, in concert with gas chromatography and mass spectrometry, it was determined three decades ago that cutin's major monomeric constituents are $C_{16}$ hydroxylated fatty acids (Kolattukudy, 1984; Holloway, 1982b). Nonetheless, this biopolymer's insolubility has made it challenging to elucidate the detailed molecular architecture responsible for its support and defense functions.

In recent years, partial degradation of tomato and lime fruit cutin either by enzymatic or chemical means has been used to generate soluble oligomeric products that retain essential covalent connections from the native plant polyester (Stark and Tian, 2006). In addition, cross-polarization magic-angle spinning (CPMAS) $^{13}C$ NMR experiments on intact cutin and suberin have served to identify the major functional groups in both biopolymers and to establish the cross-link sites and polymeric domain structures. CPMAS $^{13}C$ NMR techniques have also been used to obtain molecular-scale structural and dynamic information on bulk solid

* Corresponding author. Address: Department of Chemistry, City College of New York, City University of New York Graduate Center and Institute for Macromolecular Assemblies, New York, NY 10031, USA. Tel.: +1 212 650 8916; fax: +1 212 650 8719.
*E-mail address:* stark@sci.ccny.cuny.edu (R.E. Stark).

0031-9422/$ - see front matter © 2008 Elsevier Ltd. All rights reserved.
doi:10.1016/j.phytochem.2008.08.016

samples of plant cuticle. For example, for those carbons that cross-polarize, $T_1(C)$ and $T_{1\rho}(C)$ relaxation experiments have been used to characterize flexibility on megahertz and kilohertz timescales, respectively, in lime-fruit cuticle. Such experiments probe local motional restrictions at polymeric covalent cross-links and cooperative main-chain undulations that may be linked to cuticular resiliency (Garbow and Stark, 1990).

Chemical and mechanical stresses and environmental modulators, such as moisture and cold, can promote fracture of the cuticle, seriously compromising its protective functions. The practical consequences include microbial attack of fruits and vegetables, leading to agricultural losses estimated at greater than $10 billion per year in the United States alone (Gianessi and Reigner, 2005). In order to understand and augment the robustness of the cuticular structure, it is therefore important to characterize both thermal and mechanical properties, in bulk and on the surface itself, as a function of these environmental variables and as they relate to molecular structure. For instance, the thermal response of intact and dewaxed tomato fruit skins, as well as the cuticular waxes themselves, have been investigated by differential scanning calorimetry (DSC) (Luque and Heredia, 1997; Casado and Heredia, 2001; Matas et al., 2004). Cuticular ultrastructure has been investigated extensively with transmission and scanning electron microscopies (Kolattukudy, 1984; Holloway, 1982a). Moreover, the development of the atomic force microscope (AFM) has enabled the direct examination of the three-dimensional architecture of biological surfaces, including plant tissues and surfaces (Gould et al., 1990; Canet et al., 1996; Kirby et al., 1996; Mechaber et al., 1996; Round et al., 1996), with spatial resolutions at or near those of electron microscopy, under ambient gas or liquid environments and with little or no special preparation of the samples.

In its natural environment, the plant cuticle experiences a wide variety of hydration states. A complete understanding of cuticular function thus requires study of its thermal and mechanical properties as a function of hydration. For cutin saturated with water, the glass transition temperature ($T_g$) has been found to be reduced from 23 °C to ~16 °C (Matas et al., 2004). As $T_g$ can be viewed as the temperature above which a polymer undergoes significant segmental motion, this drop clearly indicates that water affects the mechanical behavior of the cuticle. The bulk mechanical properties of enzymatically isolated tomato cuticle have also been characterized directly over the temperature range 10–45 °C and relative humidity of 40%-to-wet, with specific measurement of tensile modulus, breaking strength, and maximum elongation (Matas et al., 2005). Temperature and humidity were both found to have important effects on the stiffness and strength of the tomato cuticle, whereas the maximum elongation-to-break remained approximately constant. Finally, AFM has been used to investigate the surface mechanical properties of isolated, dewaxed tomato fruit cuticles as a function of their hydration state (Round et al., 2000). Dramatic changes in surface elastic modulus were observed with even modest water uptake, in reasonable accord with previously reported variations in bulk elastic modulus (Petracek and Bukovac, 1995).

Previous NMR studies of synthetic and naturally-occurring polymers and biopolymers have demonstrated the sensitivity of NMR relaxation parameters to hydration (Ganapathy et al., 1986; Jackson and Bryant, 1989; Willis and Herring, 1987; Horii et al., 1987; Kennedy and Bryant, 1990). In poly(vinyl acetate), hydration caused a dramatic decrease in carbon spin–lattice relaxation ($T_1(C)$), which is dominated by the high-frequency motion of $H_2O$ (but not $D_2O$) molecules (Ganapathy et al., 1986). Much smaller effects of water addition were observed on $T_{1\rho}(H)$, $T_{1\rho}(C)$ and the carboxyl-carbon chemical-shift tensor, all of which are dominated by slower polymer motions. In glycogen, a branched glucose polymer, addition of water reduced the $^{13}C$ spin–lattice relaxation times by two orders of magnitude over the range 7–70% water, with a concomitant decrease in proton–carbon dipolar couplings (Jackson and Bryant, 1989). These latter results were interpreted in terms of water producing a dramatic increase in local polymer-chain motions. By contrast, hydration of the protein lysozyme caused a significant narrowing in spectral linewidths that was not commensurate with loss of proton–carbon dipolar coupling or major changes in the relaxation parameters characterizing cross-polarization (Kennedy and Bryant, 1990). Instead, water appeared to decrease the distribution of local conformations sampled by the protein, decreasing the observed linewidths. These studies illustrate the wide range of changes observed in macromolecules in response to increasing levels of hydration.

Two studies of fruit cuticles at extremes of temperature have appeared in the literature. Using dewaxed tomato cutin hydrated with 1% by weight $D_2O$, we found two slowly exchanging water populations of differing order and mobility at plausible growing temperatures from −10 to +35 °C (Stark et al., 2000). More recently, Sachleben et al., (2004) reported a continuous increase in $(CH_2)_n$ linewidths as the temperature was lowered from room temperature, indicating that polymer-chain motions are progressively frozen out from room temperature down to −93 °C.

In this manuscript, we report the results of a comprehensive $^{13}C$ NMR relaxation study of intact, hydrated tomato cuticle aimed at providing insights into the changes in cuticular structure and dynamics induced by $D_2O$ hydration and thermal variations. High frequency polymer-chain motions are probed by measurement of $T_1(C)$, whereas lower frequency motions are investigated through measurement of $T_{1\rho}(H)$ and $T_{1\rho}(C)$ and by measurement of the relative fraction of signals observed in cross-polarization experiments with high-power (dipolar) decoupling and direct-polarization experiments with low-power (scalar) decoupling (DPMAS). Results of these experiments are interpreted in terms of changes occurring in individual polymer motions of the cutin/wax components of tomato cuticle and in the interaction of these components in intact cuticle in response to the addition of water. In a separate series of experiments, variable-temperature measurements of $T_1(C)$ and $T_{1\rho}(C)$ for dry tomato cuticles are used to evaluate the impact of temperature stress on biomacromolecular dynamics on different timescales. The possible functional consequences of these cuticular alterations are also discussed.

## 2. Results and discussion

### 2.1. Effects of hydration on proportions of mobile and immobile carbons

Fig. 1 (bottom trace) shows a typical CPMAS $^{13}C$ NMR spectrum of hydrated tomato fruit cuticles, which bears an overall resemblance to those reported previously for lime and tomato fruit cutins, but has fewer aromatic signals than the lime materials (Garbow and Stark, 1990; Round et al., 2000; Batteas and Stark, 2005). Prominent resonances are attributable to long-chain methylene groups ($(CH_2)_n$, 20–40 ppm), oxygen-linked aliphatic carbons (CHO and $CH_2O$, 60–80 ppm), and carbonyl groups (C═O, 165–180 ppm), as expected based on its major 10,16-dihydroxyhexadecanoic acid monomeric constituent (Holloway, 1982b; Osman et al., 1995, 1999). Although the cutin biopolyester is expected to be the predominant contributor to the spectrum, wax methylenes and residual cell-wall polysaccharides may also account for some of the NMR signal intensity at 33, 60–80, and 100–110 ppm.

Fig. 1 also illustrates the $^{13}C$ NMR spectra obtained with CPMAS and high-power $^1H$ decoupling (bottom) compared with DPMAS and low-power decoupling (top). The integrated CPMAS $^{13}C$ NMR signal intensities were corrected for cross-polarization efficiencies and finite CP contact times, whereas the DPMAS spectra were

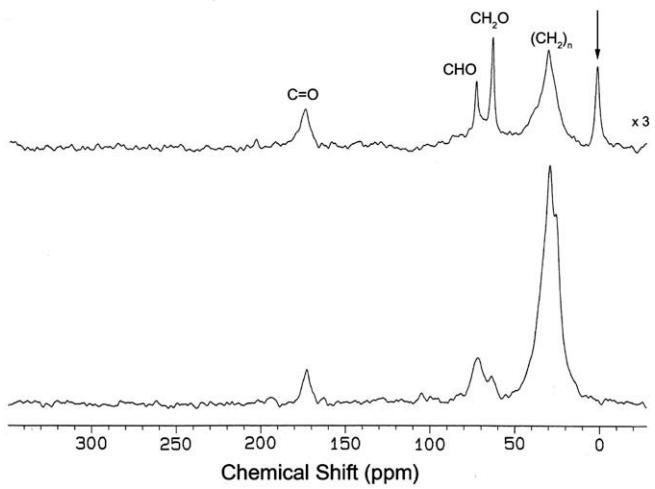


**Fig. 1.** 31.94 MHz MAS $^{13}C$ NMR spectra of a wet tomato cuticle preparation (42% $D_2O$ by weight) acquired at 298 K with 3.0-kHz spinning by two methods: top, direct polarization (DP) with 5-kHz $^{1}H$ decoupling applied only during the acquisition period, a recycle delay of 3 s, and 25,000 transients; bottom, cross polarization (CP) with 2-ms contact time and $^{1}H$ rf fields of 50 and 65 kHz applied during Hartmann–Hahn mixing and signal acquisition times, respectively, a recycle delay of 1.5 s, and 16,000 transients. The data were normalized according to the number of transients collected, and the vertical scale of the DP spectrum was then expanded threefold to facilitate visual comparisons. The arrow in the DP spectrum designates a peak originating from the sample rotor.

measured without $^{13}C\{^{1}H\}$ nuclear Overhauser enhancements (Garbow and Stark, 1990), enabling estimation of the rigid and mobile populations of each major carbon type as a function of water exposure. Those segments in solid polymers that reorient at rates exceeding $\sim 10^5$ Hz exhibit strong $^{13}C$ NMR signals even with direct polarization and under low-power $^{1}H$ decoupling conditions (Zlotnik-Mazori and Stark, 1988; Jelinski et al., 1981). Table 1 compares the resulting proportions for dry, damp, and wet tomato cuticle samples, both with and without native waxes.

As a group, these NMR spectroscopic data for tomato materials serve first to extend our prior findings for limes (Garbow and Stark, 1990): in the dry state, a high proportion of the chain methylene carbons is motionally constrained when waxes are integrated with the cuticular netting. The results, summarized in Table 1, also test

**Table 1**
Solid-like carbons in fruit cuticles

| Sample | Proportion of rigid carbons (%)[a] in specified chemical shift range (ppm)[b] | | |
|---|---|---|---|
| | 20–40 | 60–80 | 160–180 |
| *Lime* | | | |
| Dry cutin[c] | 41 | – | – |
| Dry cuticle[c] | 78 | – | – |
| *Tomato* | | | |
| Driest cuticle[d] | 90 | 85 | 75 |
| 1.5% damp[e] | 85 | 82 | 82 |
| 42% wet[e] | 76 | 37 | 37 |

[a] From comparison of integrated intensities in CPMAS data (extrapolated to zero contact time and adjusted for CP enhancement) and DPMAS spectra (acquired without $^{13}C\{^{1}H\}$ nuclear Overhauser effect), both acquired at ambient temperature (Garbow and Stark, 1990). Uncertainties in determination of the intensities are estimated as 15%.

[b] The $^{13}C$ chemical shift ranges correspond to chain methylenes ($(CH_2)_n$), oxygen-linked aliphatics ($CH_2O$ and CHO), and carbonyls (C=O), respectively. Overlapped cutin and wax $(CH_2)_n$ peaks are treated together.

[c] From Garbow and Stark, (1990).

[d] Dried to constant mass in a SpeedVac apparatus. The CP enhancement measured for dry lime fruit cuticle was used in calculations for this tomato sample.

[e] Equilibrated above supersaturated salt solutions and designated according to the percent by weight of $D_2O$ in the hydrated cuticular tissue.

whether cuticular interactions with water are accompanied by increases in the liquid-like proportion of particular carbon moieties. As compared with dewaxed tomato cutin samples for which $^{1}H$ NMR linewidths of the bulk methylene groups in wideline separation experiments showed a plasticizing effect associated with exposure to water (Round et al., 2000), those groups in cuticles containing epicuticular waxes remain largely solid-like. Nonetheless, the increases in rapid segmental motions at these and other sites are correlated with threefold reductions in the bulk modulus reported for a set of nominally similar tomato cuticle samples (Batteas and Stark, 2005). A link between such dynamic and functional changes has been proposed previously for synthetic polymeric materials (North, 1975).

Among the various functional groups, the bulk methylenes maintain the highest proportions of rigid carbons in each tomato sample despite the presence of potentially flexible polymeric chains in tomato cutin's predominant 10,16-dihydroxyfatty acid monomeric constituent (Holloway, 1982b; Osman et al., 1995, 1999). This finding is attributable to strong hydrophobic interactions between cutin aliphatic chains and the waxes, which are more favorable energetically than interactions with water. The fluidizing effect on the fruit's protective covering appears most pronounced at oxymethylene, oxymethine, and carbonyl sites (60–80 and 160–180 ppm), making the corresponding resonances very prominent in the $^{13}C$ DPMAS NMR spectrum (Fig. 1, top). The $CH_2OC(O)R$ resonance at ~63 ppm displays especially strong, sharp DP NMR signals. Our hypothesis is that some inter-chain hydrogen-bond interactions within the dry biopolymer are replaced by transient hydrogen bonds between water protons and these oxygen-containing structural moieties, allowing for greater segmental flexibility.

Quantitatively, the results show a roughly twofold preferential enhancement of motional freedom for the $CH_nO$ and C=O groups upon complete hydration, but significant across-the-board fluidizing effects only for very wet samples. Conversely, it is clear that $(CH_2)_n$ signals, which include contributions from both the underlying cutin biopolymer (~90%) and the epicuticular waxes (~10%), show a more modest diminution of the rigid spectral component even in very wet tomato cuticular materials. The latter trend, which is supported by the invariant average $^{1}H$ linewidths observed in wideline separation spectra of a similar series of tomato fruit samples (Batteas and Stark, 2005), suggests that many of the aliphatic chains of the cutin structural support are effectively shielded from the plasticizing effects of water by the waxy overlayer even though the material as a whole exhibits a threefold smaller resistance to deformation (bulk modulus) when hydrated (Batteas and Stark, 2005).

### 2.2. Hydration effects on local flexibility of carbons that cross-polarize

For the subpopulation of solid-like carbons i.e., those which cross-polarize efficiently and require high-power $^{1}H$ decoupling to give well-resolved spectral lines, the NMR spin–lattice relaxation $T_1(C)$ results presented in Table 2 offer a more detailed view of local motional behavior occurring at ~30 MHz rates. Thus, in addition to classifying the various carbon segments as mobile and rigid, it is possible to focus on the high-frequency dynamic response of different solid-like functional groups to hydration stress. For the dry reference state, the aliphatic-chain methylenes show a substantial degree of flexibility (short relaxation times) compared with the anchoring $CH_nO$ and C=O groups in lime and tomato cuticular samples (Garbow and Stark, 1990; Batteas and Stark, 2005).

As the cuticles become hydrated and an increasing portion of the carbon population becomes mobile enough to be observed by DPMAS $^{13}C$ NMR spectroscopy with low-power decoupling, it might be expected that the remaining solid-like moieties are more

**Table 2**
$^{13}C$ spin–lattice relaxation parameters for cross polarizable carbons in fruit cuticles

| Sample | Resonance frequency | <$T_1$(C)>, s[a] | | | |
|---|---|---|---|---|---|
| | | Carbon type | | | |
| | | $(CH_2)_n$ | $CH_2OCOR$ | CHOCOR, CHOH | C=O |
| *Lime* | | | | | |
| Dry cutin[b] | 32 MHz | 0.20 | 0.24 | ~5.0 | ~4.6 |
| Dry cutin[b] | 50 MHz | 0.19 | 0.19 | ~5.6 | ~2.3 |
| Dry cuticle[b] | 50 MHz | 0.13 | 0.10 | ~2.0 | ~1.1 |
| *Tomato* | | | | | |
| Dry cuticle[c] | 75 MHz | 0.31 | – | – | – |
| 1.5% damp | 32 MHz | 0.36 | – | 5.5 | 6.0 |
| 42% wet | 32 MHz | 0.20 | 0.16 | 2.2 | 5.4 |

[a] Average values derived from the semilogarithmic dependence of $^{13}C$ signal heights on recovery times between 0 and ~200 ms (if $T_1$ <1 s); between 0 and 2.5 s (if $T_1$ >1 s). A rapidly recovering component of the CHO signal is also present. These measurements have typical uncertainties of 10% for the strong $(CH_2)_n$ signals, 25% for the remaining resonances. All measurements were conducted at ambient temperature, estimated as 295 K.
[b] From Garbow and Stark (1990); the value quoted for the $(CH_2)_n$ is a weighted average obtained from the resonances at 29 and 33 ppm, which were measured separately.
[c] From Batteas and Stark (2005), using a weighted average obtained from the resonances at 29 and 33 ppm for the $(CH_2)_n$ groups. The sample was air dried.

motionally constrained. However, the significant drops in $T_1$(C) – including $(CH_2)_n$, $CH_nO$, and C=O carbons – demonstrate the substantial fluidizing impact of hydration interactions. As found with the proportions of mobile moieties (Table 1), the $T_1$(C) values change most for $CH_nO$ groups that can hydrogen bond to water (factor of 2.5), but they are also significant (factor of 1.8) for the rigid portion of bulk methylene carbons. The spin–lattice relaxation is likely dominated by modulation of the directly-bonded C–H interactions of the biopolymer rather than high-frequency water motions, since the small gyromagnetic ratio of deuterons in $D_2O$ will attenuate the latter effects (Ganapathy et al., 1986).

A plausible physical picture that accommodates both the small decrease in cross-polarizable $(CH_2)_n$'s and their more efficient carbon spin–lattice relaxation is as follows. Interactions with waxes attenuate the plasticizing effects on most of the methylenes sufficiently to prevent DP observation with low-power decoupling. Nonetheless, those $(CH_2)_n$'s located within a few bonds of the hydrophilic $CH_nO$ groups gain some local flexibility and undergo more rapid spin–lattice relaxation (i.e., they have shorter values of $T_1$(C)). As noted above, a possible molecular explanation for these trends invokes replacement of hydrogen-bonding interactions among polymeric chains with transient water interactions that allow for greater flexibility of the nearby carbon segments. In terms of biomechanical consequences, the added mobility of the solid-like carbon segments once again correlates with an observed threefold drop in bulk modulus (Batteas and Stark, 2005).

### 2.3. Polymeric domains and overall flexibility of hydrated cuticles

Once again considering the subpopulation of rigid carbons that cross polarizes efficiently and requires high-power $^1H$ decoupling to give well-resolved spectral lines, the spin relaxation results presented in Table 3 offer a complementary view of cuticular domain organization and cooperative overall chain dynamics. These properties have been proposed as essential to fruit cuticular toughness and resiliency (Round et al., 2000). The dispersion of the relaxation time $T_{1\rho}$(H), measured independently through the cross-polarization behavior of the various carbon resonances, tests whether dipole–dipole couplings between the various proton types are sufficiently strong to establish a common spin reservoir. In practice, $^1H$ nuclei that are motionally rigid and located within ~5 nm of one another are considered to be 'intimately mixed' and will exhibit a common value of <$T_{1\rho}$(H)>. In addition, the numerical values of this relaxation time reflect the prevalence of dynamic processes that occur at a rate corresponding to the spin–lock field strength, in this instance expressed in frequency units as 50 kHz.

All of the cutin proton rotating-frame relaxation times are shorter than reported for lignin, cellulose, and typical synthetic polymers (Schaefer and Stejskal, 1979; Haw et al., 1984), reflecting greater mid-kHz motions in fruit cuticular biopolymers. As compared with lime cuticles, the results for 1.5% damp tomato samples most closely match the dry lime cuticle; in both cases the values become progressively longer in the series from $(CH_2)_n$ to $CH_nO$ to C=O carbons. For a given carbon type, the <$T_{1\rho}$(H)>'s increase by factors ranging from 1.7 to 2.7 as the cuticles become fully hydrated. Moreover, the normalized standard deviation of these values is also diminished for wet tomato samples, matching the convergence observed in dry lime cuticles and indicating almost complete spin diffusion and uniform mixing of the protons on the 5-nm distance scale.

**Table 3**
$^1H$ rotating-frame relaxation times for cross polarizable carbons in fruit cuticles

| Sample | <$T_{1\rho}$ (H)>[a], ms | | | | | | |
|---|---|---|---|---|---|---|---|
| | Carbon type | | | | | | |
| | $(CH_2)_n$ | $CH_2OCOR$ | CHOCOR, CHOH | C=O | Avg | Std dev | Std dev/ avg |
| *Lime* | | | | | | | |
| Dry cutin[b] | 3.4 | 4.5 | 4.6 | 5.7 | 4.6 | 0.94 | 0.21 |
| Dry cuticle[b] | 3.8 | 3.8 | 4.0 | 5.4 | 4.3 | 0.78 | 0.18 |
| *Tomato* | | | | | | | |
| Driest cuticle | 2.1 | 2.9 | 3.1 | 4.9 | 3.2 | 1.2 | 0.37 |
| 1.5% damp | 3.2 | – | 3.6 | 5.2 | 3.9 | 1.1 | 0.28 |
| 42% wet | 5.7 | 7.5 | 6.7 | 8.1 | 7.0 | 1.0 | 0.15 |

[a] Average values derived from the dependence of $^{13}C$ signal heights vs. cross-polarization time (1.0–4.0 ms), obtained at ambient temperature. These measurements have estimated uncertainties of 5–15%.
[b] Garbow and Stark (1990).

**Table 4**
$^{13}$C rotating-frame relaxation times for cross polarizable carbons in fruit cuticles

| Sample | <$T_{1\rho}$(C)>, ms[a] | | | |
|---|---|---|---|---|
| | Carbon type | | | |
| | $(CH_2)_n$ | $\boldsymbol{C}H_2OCOR$ | $\boldsymbol{C}HOCOR$, CHOH | C=O |
| *Lime* | | | | |
| Dry cutin[b] | 3.3 | 5.3 | 12.4 | |
| Dry cuticle[b] | 2.8 | 3.6 | 7.5 | |
| *Tomato* | | | | |
| Driest cuticle | 2.1 | – | ~4.4 | |
| 0.2% damp | 1.9 | ~7.8 | ~6.5 | |
| 55% wet | 3.2 | – | ~5.5 | ~9.5 |

[a] From the short-time behavior (0.05–1.00 ms) of $^{13}$C magnetization held in a 50-kHz field after spin locking and cross polarization from $^{1}$H, observed at ambient temperature. The spin-relaxation parameters have estimated uncertainties of 5% for the $(CH_2)_n$ peak and 20% for all others.
[b] From Garbow and Stark (1990).

These results suggest that in dry and damp tomato cuticular samples for which distinct values of $T_{1\rho}$(H) are observed across each spectrum, mid-kHz motions are most prevalent at the long-chain aliphatic sites and least efficient at the carbonyl anchoring groups. That hypothesis is confirmed by trends for $T_{1\rho}$(C) in a set of nominally similar samples (Table 4); spin diffusion among carbons is not a concern, so the relaxation parameters report on mid-kHz motions directly. However, in wet samples for which the spins are well mixed and the relaxation times converge, the longer common value of $T_{1\rho}$(H) indicates diminished motions at rates near 50 kHz for the solid-like constituents. Because rigidity enhances spin communication, interactions with water impact all molecular sites when viewed in a $T_{1\rho}$(H) experiment. Thus, the slow collective motions of the solid-like population of cuticular carbons become less prevalent in very wet environments, even as values of $T_{1\rho}$(C) reveal a gradient of increasing constraints from $(CH_2)_n$ to $CH_nO$ to C=O sites. From a functional point of view, the loss of mid-kHz spectral density for the cross-polarizable carbons may be correlated with diminished mechanical impact strength of the polymeric layer or compromised cuticular toughness (Schaefer et al., 1977).

Examination of the average values <$T_{1\rho}$(C)> shown in Table 4 also establishes an insensitivity of these spin relaxation parameters to hydration state when viewed at both the aliphatic chain and oxymethine carbon sites. Both these magnitudes and trends are in accord with the behavior of $(CH_2)_n$ groups in dewaxed tomato cuticles (Round et al., 2000), but for the CHOCOR and CHOH

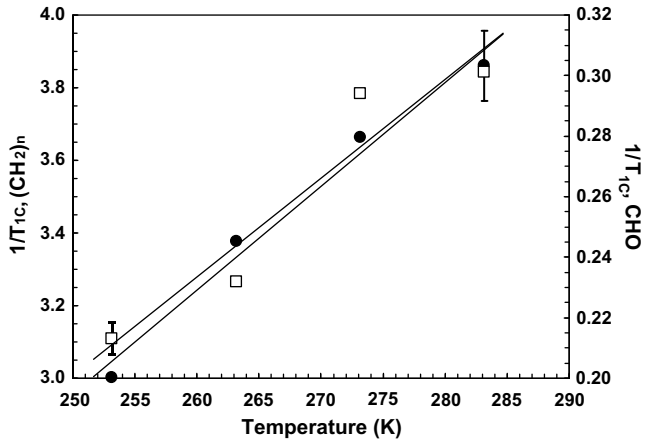


**Fig. 2.** Dependence of average spin–lattice relaxation rates (<1/$T_1$(C)>) on temperature for CHO (□) and bulk methylene (●) carbons in tomato fruit cuticles. Representative error bars are shown for the CHO data at 253 K and the $(CH_2)_n$ result at 283 K, respectively.

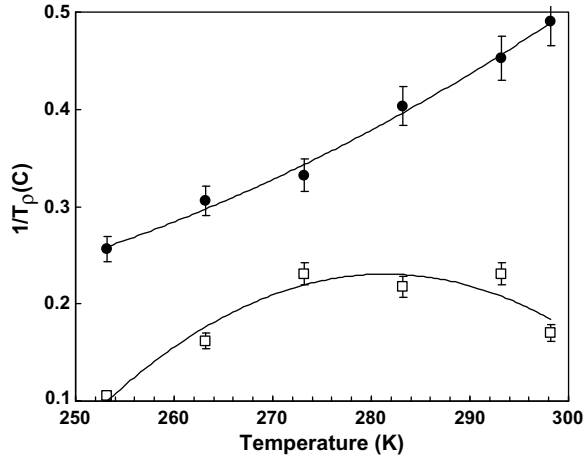


**Fig. 3.** Dependence of average rotating frame relaxation rates (<1/$T_{1\rho}$(C)>) on temperature for CHO (□) and $(CH_2)_n$ (•) carbons. The curves are drawn to guide the eye.

groups, saturation of the latter materials with water produces a 40% drop in carbon rotating-frame relaxation times. The overall picture from the rotating-frame relaxation data, then, is that collective motions are not altered to a major degree by hydration unless the cuticle is truly waterlogged and there are no waxes present to mitigate the impact of water.

### 2.4. Effects of temperature stress on cuticular flexibility

A series of carbon spin relaxation measurements was undertaken on dry tomato cuticles in order to assess the impact of extremes of temperature on cuticular dynamics and associated mechanical properties. As a preliminary model for temperature stress that might be encountered under frost conditions in the field, both $T_1$(C) and $T_{1\rho}$(C) were monitored between 253 and 298 K. In contrast to previous variable-temperature measurements on tomato cutin (Sachleben et al., 2004), no changes in $^{13}$C NMR linewidths were observed for tomato cuticles within this restricted temperature range. As expected for the cross-polarizable carbons, the spin–lattice relaxation rates drop as the temperature is lowered, indicating diminished segmental reorientation and an increase in bulk modulus. The dependence of $1/T_1$(C) on temperature (Fig. 2) is an order of magnitude more pronounced for the $(CH_2)_n$ groups, suggesting a progressive chain freezing phenomenon (Sachleben et al., 2004) that may also alter the efficacy of cutin–wax interactions. A qualitatively similar pattern of temperature-dependent changes is observed for $1/T_{1\rho}$(C) (Fig. 3): collective undulations at rates of ~50 kHz are less efficient at low temperatures though the effect is less dramatic for the CHO groups, perhaps as a result of cross-linking constraints. These latter trends suggest that reduced overall chain motions account for deficiencies in impact strength and a consequent tendency for fruit cracking at freezing temperatures. Taken together, the spin relaxation trends implicate cutin and/or wax aliphatic chains in changes of bulk mechanical properties that may compromise the robustness of the tomato fruit cuticle under thermal stress conditions.

## 3. Conclusions

In this study, a battery of NMR spin relaxation experiments have been used to investigate how hydration and temperature stress impact the dynamics of tomato fruit cuticles on diverse frequency scales and at particular molecular sites. Drawing on the known responsiveness of relaxation parameters to hydration effects (Ganapathy et al., 1986; Jackson and Bryant, 1989; Willis

and Herring, 1987; Horii et al., 1987; Kennedy and Bryant, 1990), we have probed motional characteristics associated with (bio)polymer mechanical properties such as bulk modulus, impact strength, and toughness, seeking trends that illuminate the molecular factors responsible for maintaining fruit cuticular integrity under these environmental stress conditions.

Whereas hydration of dewaxed tomato cuticles plasticizes the bulk materials, the surface layer, and diverse molecular groups (Round et al., 2000), in native cuticles the increase in local motions ($10^5$–$10^8$ Hz) is most pronounced for hydrophilic $CH_nO$ moieties. These findings suggest a physical model in which inter-chain hydrogen bonds are replaced by transient aqueous interactions but strong hydrophobic interactions are maintained between aliphatic chains of the cutin and wax constituents. Concurrently, the hydration-induced drop in bulk modulus is just threefold for waxy tomato cuticular samples, compared with sixfold for the dewaxed samples (Batteas and Stark, 2005). Exposure to water also promotes rigidity and efficient spin communication that may be correlated with diminished cuticular impact strength, but no site-specific motional sensitivity was found for the slower overall motions (50 kHz). Although a lowering of the temperature produces the expected diminution of segmental and overall reorientation for both the solid-like $(CH_2)_n$ and $CH_nO$ groups, the impact on the aliphatic chains may be sufficiently pronounced to compromise the efficacy of cutin–wax interactions necessary to maintain a robust cuticular barrier. Taken together, these findings illustrate the exquisitely tuned ability of plant cuticles to adjust to hydration and temperature stresses imposed by their environment.

## 4. Experimental

### 4.1. Cuticle from tomatoes

Ripe red tomatoes (*Lycopersicon esculentum*) were purchased locally during the summer months; their skins were removed in large sections and soaked in distilled $H_2O$ for 30 min. Following published procedures (Pacchiano et al., 1993), pectin was removed by immersing the cuticular sheets in a 4 mg/ml solution of *Aspergillus niger* pectinase (Sigma Chemical Company, St. Louis, MO) in a 50 mM, pH 4, NaOAc buffer, then shaking gently for three days in a thermostatted incubator at 31°C (New Brunswick Scientific, Edison, NJ). The cuticles were dried in air for several hours and then to constant mass in a SpeedVac apparatus (Thermo Savant Instruments, Holbrook, NY).

Hydration of the cuticles was achieved by equilibrating the 200-mg cuticular samples in closed thermostatted containers above supersaturated $D_2O$ solutions of various inorganic salts. In addition to pure $D_2O$, $CaCl_2$, $CuSO_4$, $Na_2Cr_2O_7$, and LiCl were chosen to span a wide range of relative humidities (Weast, 1983) and permit parallel evaluation of water order and motion (Stark et al., 2000). Two alternate protocols were used: (a) sheets were placed on a gauze net suspended from the center of the lid; and (b) sheets were placed in a dry test tube which was then immersed in the desired salt solution. After 5 days at 20 °C, the samples were reweighed to determine the percent hydration; typically 60–160 mg samples were then loaded immediately into plastic inserts for NMR studies.

### 4.2. NMR spectroscopy

NMR experiments were performed on either of two spectrometers: a Varian NMR Instruments (Palo Alto, CA) Unity*plus*-300 instrument operating at a proton Larmor frequency of 300 MHz and a home-built instrument operating at a proton Larmor frequency of 127 MHz. Cross-polarization magic-angle spinning (CPMAS) $^{13}C$ NMR spectra were obtained at 31.94 MHz and 298 K using 2-ms, 50-kHz $^{13}C$–$^{1}H$ spin–lock contacts, high-power (65 kHz) proton decoupling and magic-angle spinning at a speed of 3.0 kHz. A recycle delay of 1.5 s was inserted between successive data acquisitions. Samples were sealed in small, screw-top Kel-F containers prior to all NMR experiments. In the case of hydrated samples, these Kel-F containers were equipped with O-ring seals to assure that a constant moisture level and mass were maintained throughout the experiments. For rotating-frame relaxation measurements, contact times and rf field strengths were varied as described below.

Direct-polarization magic-angle spinning (DPMAS) $^{13}C$ NMR spectroscopic data were acquired at 31.94 MHz following a single $^{13}C$ 90° pulse. A frequency-modulated, continuous wave $^{1}H$ decoupling field of 5 kHz was used and the recycle delay between acquisitions was 3 s, >5 times the spin–lattice relaxation time for methylene carbons.

### 4.3. Spin-relaxation measurements

Proton rotating-frame relaxation times, $T_{1\rho}(H)$, were determined from the decay of the carbon signal as a function of $^{13}C$–$^{1}H$ contact time ($\tau$) in a CPMAS experiment (Stejskal et al., 1979). The $\langle T_{1\rho}(H)\rangle$ values were calculated from least-squares fits of log (carbon signal height) vs. $\tau$. Carbon spin–lattice relaxation times, $T_1(C)$, were measured by monitoring the recovery of $^{13}C$ magnetization following cross-polarization and inversion (Torchia, 1978). Values of $\langle T_1(C)\rangle$ were determined from the initial rates of this recovery. Average carbon rotating-frame relaxation times, $\langle T_{1\rho}(C)\rangle$, were measured by recording the $^{13}C$ signal as a function of carbon spin–lock time following cross-polarization. The spin–lock field, $B_1(C)$, was held at 50 kHz. Values of $\langle T_{1\rho}(C)\rangle$ were determined from a least squares fit of log (carbon signal height) vs. spin–lock time over the first 1.0 ms of signal decay (Schaefer and Stejskal, 1979). Variable temperature spin-relaxation experiments were conducted on the Unity*plus*-300 instrument using a Varian temperature regulator; temperatures were estimated (±1 °C) from measurements of $^{1}H$ chemical shifts in liquid ethylene glycol.

## Acknowledgements

We thank Dr. Patrick J. O'Connor, Mr. Frank Corrigan, Mr. Mark Werner, Ms. Rama Raguthu, and Mr. Mohamed Al-Bashir for assistance in the preparation of cuticular samples and acquisition of NMR spectroscopic data. This work was supported by a grant (to R.E.S.) from the National Science Foundation (MCB-0134705). The 300 MHz NMR spectrometer was supported by the College of Staten Island and the CUNY Institute for Macromolecular Assemblies, a Center of Excellence of the Generating Employment through New York State Science program. S.M.S.-F. and F.C. were participants in NSF's Research Experiences for Undergraduates program; P.J.O. was the recipient of an NSF Research Opportunity Award.

## References

Bargel, H., Koch, K., Cerman, Z., Neinhuis, C., 2006. Structure–function relationships of the plant cuticle and cuticular waxes – a smart material? Funct. Plant Biol. 33, 893–910.

Batteas, J.D., Stark, R.E., 2005. Surface and interfacial studies of plant biopolymers. In: Chen, P. (Ed.), Molecular Interfacial Phenomena of Polymers and Biopolymers. Abington Hall, Woodhead Publishing Co., Cambridge, UK, pp. 580–608.

Canet, D., Rohr, R., Chamel, A., Guillain, F., 1996. Atomic force microscopy study of isolated ivy leaf cuticles observed directly and after embedding in Epon. New Phytol. 134, 571–577.

Casado, C.G., Heredia, A., 2001. Self-association of plant wax components: a thermodynamic analysis. Biomacromolecules 2, 407–409.

Ganapathy, S., Chacko, V.P., Bryant, R.G., 1986. Poly(vinyl acetate) dynamics studied by proton and carbon-13 nuclear magnetic resonance in the solid state. Macromolecules 19, 1021–1029.

Garbow, J.R., Stark, R.E., 1990. Nuclear magnetic resonance relaxation studies of plant polyester dynamics 1. Cutin from limes. Macromolecules 23, 2814–2819.
Gianessi, L.P., Reigner, N., 2005. The value of fungicides in U.S. Crop production. Publ. No. 1-243.
Gould, S.A.C., Drake, B., Prater, C.B., Weisenhorn, A.L., Manne, S., Kelderman, G.L., Butt, H.J., Hansman, H., Hansma, P.K., 1990. The atomic force microscopy: a tool for science and industry. Ultramicroscopy 33, 93–98.
Haw, J.F., Maciel, G.E., Schroeder, H.A., 1984. Carbon-13 NMR spectrometric study of wood and wood pulping with cross polarization and magic-angle spinning. Anal. Chem. 56, 1323–1329.
Heredia, A., 2003. Biophysical and biochemical characteristics of cutin, a plant barrier biopolymer. Biochim. Biophys. Acta 1620, 1–7.
Holloway, P.J., 1982a. Structure and histochemistry of plant cuticular membranes: an overview. Linnean Soc. Symp. Ser. 10, 1–32.
Holloway, P.J., 1982b. The chemical constitution of plant cutins. In: Cutler, D.F., Alvin, K.L., Price, C.E. (Eds.), The Plant Cuticle. Academic Press, New York. pp. 45–85.
Horii, F., Hirai, A., Kitamaru, R., 1987. CP/MAS$^{13}$ C NMR spectra of the crystalline components of native celluloses. Macromolecules 20, 2117–2120.
Jackson, C.L., Bryant, R.G., 1989. Carbon-13 NMR of glycogen: hydration response studied by using solids methods. Biochemistry 28, 5024–5028.
Jelinski, L.W., Schilling, F.C., Bovey, F.A., 1981. Carbon-13 nuclear magnetic resonance studies of solid segmented copolymers 1. Mobile domains of a polyester thermoplastic elastomer. Macromolecules 14, 581–586.
Kennedy, S.D., Bryant, R.G., 1990. Structural effects of hydration: studies of lysozyme by $^{13}$C solids NMR. Biopolymers 29, 1801–1806.
Kirby, A.R., Gunning, A.P., Waldron, K.W., Morris, V.J., Ng, A., 1996. Visualization of plant cell walls by atomic force microscopy. Biophys. J. 70, 1138–1143.
Kolattukudy, P.E., 1984. Biochemistry and function of cutin and suberin. Can. J. Bot. 62, 2918–2933.
Luque, P., Heredia, A., 1997. The glassy state in isolated cuticles: differential scanning calorimetry of tomato fruit cuticular membranes. Plant Physiol. Biochem. 35, 251–256.
Matas, A.J., Cuartero, J., Heredia, A., 2004. Phase transitions in the biopolyester cutin isolated from tomato fruit cuticles. Thermochim. Acta 409, 165–168.
Matas, A.J., Lopez-Casado, G., Cuartero, J., Heredia, A., 2005. Relative humidity and temperature modify the mechanical properties of isolated tomato fruit cuticles. Am. J. Bot. 92, 462–468.
Mechaber, W.L., Marshall, D.B., Mechaber, R.A., Jobe, R.T., Chew, F.S., 1996. Mapping leaf surface landscapes. Proc. Natl. Acad. Sci. 93, 4600–4603.
North, A.M., 1975. Molecular Behavior and the Development of Polymeric Materials. Wiley, New York.
Osman, S.F., Gerard, H.C., Fett, W.F., Moreau, R.A., Dudley, R.L., 1995. Method for the production and characterization of tomato cutin oligomers. J. Agric. Food Chem. 43, 2134–2137.
Osman, S.F., Irwin, P.L., Fett, W.F., O'Connor, J.V., Parris, N., 1999. Preparation, isolation, and characterization of cutin monomers and oligomers from tomato peels. J. Agric. Food Chem. 47, 799–802.
Pacchiano, R.A., Sohn, W., Chlanda, V.L., Garbow, J.R., Stark, R.E., 1993. Isolation and spectral characterization of plant cuticle polyesters. J. Agric. Food Chem. 41, 78–83.
Petracek, P.D., Bukovac, M.J., 1995. Rheological properties of enzymatically isolated tomato (*Lycopersicon esculentum* Mill) fruit cuticle. Plant. Physiol. 109, 675–679.
Round, A.N., Kirby, A.R., Morris, V.J., 1996. Collection and processing of AFM images of plant cell walls. Microsc. Anal., 33–35.
Round, A.N., Yan, B., Dang, S., Estephan, R., Stark, R.E., Batteas, J.D., 2000. The influence of water on the nanomechanical behavior of the plant biopolyester cutin as studied by AFM and solid-state NMR. Biophys. J. 79, 2761–2767.
Sachleben, J.R., Chefetz, B., Deshmukh, A.P., Hatcher, P.G., 2004. Solid-state NMR characterization of pyrene-cuticular matter interactions. Environ. Sci. Technol. 38, 4369–4376.
Schaefer, J., Stejskal, E.O., 1979. High-resolution $^{13}$C NMR of solid polymers. Top. Carbon-13 NMR Spectrosc. 3, 283–324.
Schaefer, J., Stejskal, E.O., Buchdahl, R., 1977. Magic-angle $^{13}$C NMR analysis of motion in solid glassy polymers. Macromolecules 10, 384–405.
Stark, R.E., Tian, S., 2006. The cutin biopolymer matrix. In: Riederer, M., Müller, C. (Eds.), Biology of the Plant Cuticle. Blackwell Publishing Co., Oxford, UK. pp. 126–144.
Stark, R.E., Yan, B., Ray, A.K., Chen, Z., Fang, X., Garbow, J.R., 2000. NMR studies of structure and dynamics in fruit cuticle polyesters. Solid State NMR 16, 37–45.
Stejskal, E.O., Schaefer, J., Steger, T.R., 1979. High-resolution $^{13}$C nuclear magnetic resonance in solids. Faraday Symp. Chem. Soc. 13, 56–62.
Torchia, D.A., 1978. The measurement of proton-enhanced carbon-13 $T_1$ values by a method which suppresses artifacts. J. Magn. Reson. 30, 613–616.
Weast, R.C., 1983. CRC Handbook of Chemistry and Physics. CRC Press, Boca Raton, FL.
Willis, J.M., Herring, F.G., 1987. Effect of water in the $^{13}$C CP/MAS NMR spectrum of white spruce wood. Macromolecules 20, 1554–1556.
Zlotnik-Mazori, T., Stark, R.E., 1988. Nuclear magnetic resonance studies of cutin, an insoluble plant polyester. Macromolecules 21, 2412–2417.